

See discussions, stats, and author profiles for this publication at: <https://www.researchgate.net/publication/323335391>

Multiscale remote sensing of urbanization in Ho Chi Minh city, Vietnam – A focused study of the south

Article in *Applied Geography* · March 2018

DOI: 10.1016/j.apgeog.2017.12.026

CITATIONS

2

READS

306

3 authors:



Tuong Thuy Vu

Hoa Sen University

66 PUBLICATIONS 590 CITATIONS

[SEE PROFILE](#)



Pham Thi Mai Thy

Vietnam National Space Center (VNSC)

15 PUBLICATIONS 33 CITATIONS

[SEE PROFILE](#)



Nguyen Dao Lam

Vietnam National Space Center

30 PUBLICATIONS 290 CITATIONS

[SEE PROFILE](#)

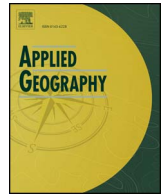
Some of the authors of this publication are also working on these related projects:



Remote Sensing Services on the Cloud [View project](#)



Agricultural information system in the Mekong Delta of Vietnam [View project](#)



Multiscale remote sensing of urbanization in Ho Chi Minh city, Vietnam - A focused study of the south

Tuong-Thuy Vu^{a,b,*}, Pham Thi Mai Thy^c, Lam Dao Nguyen^c

^a Faculty of Science and Engineering, Hoa Sen University, Ho Chi Minh City, Viet Nam

^b School of Environmental and Geographical Sciences, University of Nottingham, Malaysia Campus, Malaysia

^c Ho Chi Minh City Space Technology Application Center (STAC), Vietnam National Space Center (VNSC), Viet Nam

ARTICLE INFO

Keywords:

Remote sensing
Multi-scale
Urbanization

ABSTRACT

This study focuses on monitoring and mapping the urbanization process in the south of Ho Chi Minh City, Vietnam. Among the most vulnerable cities worldwide due to climate change, Ho Chi Minh city is experiencing the fast urbanization in last decades, especially in the south, a wetland area. The severe environmental impact such as flood has occurred more frequently implying the critical infrastructures development is far behind the expansion of newly built-up residences and hence, growing population. To what extent, the newly built-up areas have contributed to accelerating the environmental impacts in the context of climate change? The aim of this study is twofold. Firstly, we experiment three different levels of spatial resolution, sub-meter, 2.5 m and 10–15 m in mapping the landcover changes of a selected typical fast urbanization area in 2000–2010. With all about 80% classification accuracy achievement, we found that sub-meter resolution is the best for a reliable identification of land cover changes in such complex and fast-growing built-up areas whereas 2.5 m resolution is sufficient to identify the extent of built-up areas and 10–15 m is unsuitable. We also confirmed a consistent expansion, over 25%, of built-up area in our study area, using three different resolutions in spite of small differences in other landcover types. Secondly, in comparison of ground data, we revealed that most of the newly built-up areas in 2000–2010 were built on the higher land and no flood incident was recorded obviously. However, the nearby lowland experienced more floods due to the changes. A slight increase of sea level and the sinking of the city due to the groundwater extraction may also contribute to more flood incidents. Remote sensing proved to be effective in revealing the temporal urbanization and its possible consequences. However, a holistic approach to investigation needs to be developed to better understand the contribution of anthropogenic activities to environmental impacts in the climate change context.

1. Introduction

For decades, the world has experienced the acceleration of urbanization processes (UN, 2014). In the Southeast Asian region, urban land increased by 22% between 2000 and 2010 while urban populations grew over 31% (Schneider et al., 2015). Consequently, land resources are heavily exploited for growing settlements and transportation infrastructures. The development of urban areas can dramatically change the landscape along with substantial destruction to the environmental integrity (Grimm et al., 2008). Sealing the natural soil with impermeable materials such as concrete causes a strong negative impact on the urban environment and human life quality like loss of plant production and natural habitats pollution, health risks and higher social costs (Scalenghe & Marsan, 2009). In particular, the sealed soil causes more frequent flooding due to the impedance of percolation into the aquifer. The impact is obvious in Vietnam, a tropical country with the fast-growing population

and emerging economy, and accelerated as the climate is changing.

The biggest city in Vietnam, Ho Chi Minh city (HCMC), is 1 of 10 most severely impacted cities worldwide due to climate change (ADB, 2010). Being the economic hub of the country, it produces 23% of GDP, attracts 20% of foreign investment and has a population of 7 million, (over 3000 people/km²). Spreading on a lowland terrain, about 40–50% of the city area is below 1 m above sea level and another 15–20% is between 1 and 2 m. According to Asian Development Bank report (ADB, 2010), the below 1-m area will be underwater, and the 1–3 m area will be flooded by the normal tide in 2050. Land conversion due to urbanization would be the major factor in increasing urban flooding events from 356 in 2003 to 478 in 2006 (Webster, McElwee, & Worldbank, 2009).

The on-going expansion of the city to the southeast direction is sealing more wetland areas for settlements, reducing the land capacity to handle excess water. The current city drainage system is incapable of handling current water volume (Hanh, 2006) and the renovation or

* Corresponding author. Faculty of Science and Engineering, Hoa Sen University, Ho Chi Minh City, Viet Nam.
E-mail addresses: tuongthuy.vu@nottingham.edu.my, thuy.vutuong@hoasen.edu.vn (T.-T. Vu).

development of infrastructure is far behind the growth of residential areas. It seems no obvious issue in newly developed areas but the pressure bounced back to old developed areas. To bring the city planning back to a sustainable development track, there is a strong need to monitor the current urban growth process and reveal its impact in relation to climate change impacts such as frequent heavy rain, increasing temperature, etc.

Remote sensing has been extensively used in monitoring urban growth via impervious surface mapping (Weng, 2007). Medium resolution satellite images such as Landsat, which has been archived since the 70s, or SAR family is commonly used (Gómez, White, & Wulder, 2016; Lu & Weng, 2004; Van de Voorde, Jacquet, & Canters, 2011; Wieland & Pittore, 2016; Zhang, Zhang, & Lin, 2012; Zhu, 2017). Its wide extent is suitable for mapping the growth of a city as a whole but its coarse spatial resolutions (around 30-m) do not provide enough detailed information to precisely delineate the sealing of soil in a complex urban landscape with mixed pixels (Lu & Weng, 2004). To overcome this limitation, many researchers have incorporated additional information like geospatial vector data, aerial images to reach the sub-pixel details (Esch et al., 2009; Hu & Weng, 2009; Mountrakis & Luo, 2011). Alternatively, sub-meter resolution satellite images such as QuickBird, IKONOS, WorldView are used to improve the sub-pixel mapping from medium resolution images (Lu, Moran, & Hetrick, 2011; Van de Voorde et al., 2011). Moreover, these high-resolution images are suitable for deriving a detailed landuse map or mapping the details in cities such as trees, buildings (Lu, Li, & Moran, 2014; Pu & Landry, 2012; Zhang & Kerekes, 2011). Overall, data fusion is necessary to deal with complex urban landscape (Gamba, Dell'Acqua, & Dasarathy, 2005; Weng, 2012; Zhang, Zhang, & Lin, 2014).

In terms of methodology development, pixel-based classification is

the common approach for medium resolution images but it hardly deals with complex urban areas. Spectral mixture analysis (SMA) has been proved to be effective and improve the classification accuracy (Lu & Weng, 2004). However, SMA has its own issue, the impervious surface is overestimated in the small impervious surface areas or underestimated in the large impervious surface areas (Weng, 2012). With the introduction of very high-resolution satellite images, the complexity of urban areas is better revealed by applying object-based image analysis method (OBIA) approach (Blaschke, 2010). Based upon the multi-scale observation which actually mimics the human interpretation and perception, OBIA is able to represent the complexity to a multi-scale link space and hence, eventually put pixels into the context and expand the capability of multi-source data fusion. A plethora of OBIA development in last 2 decades proved that OBIA is not just simply another classification approach but a new paradigm (Blaschke et al., 2014; Ma et al., 2017). The suitability of these methods, however, should be placed in the context of the study area and the data availability towards a cost-effective mapping solution (Gamba et al., 2005; Vu, Matsuoka, & Yamazaki, 2007).

Complex growing Asian cities provide a great challenge to further improve object-based image analysis methods. Huang, Zhang, and Zhu (2014) developed a method based on morphological building index, which achieved over 80% accuracy when testing with Wuhan city (China) images. To deal with multi-sensors, Leichtle, Geiß, Wurm, Lakes, and Taubenböck (2017) proposed an object-based clustering method that successfully detected building changes in Dongying, China. In addition to new development for object-based change detection, at the level of landcover classification, there was the introduction of object-based backdating (Yu, Zhou, Qian, & Yan, 2016) and object-based semantic classification (Gu et al., 2017). Both were proved effective in



Fig. 1. The study area.

Table 1
Remote sensing data collection.

Types	Sensors	Acquisition date	Resolutions
Sub-meter	QuickBird	24 January 2003	4 multi-spectral (2.4 m) Panchromatic (0.6 m)
Sub-meter	WorldView	9 February 2010	8 multi-spectral (2 m) Panchromatic (0.5 m)
High-resolution	QuickBird	24 January 2003	4 multi-spectral (2.4 m)
High-resolution	SPOT	6 February 2009	4 multi-spectral (10 m) Panchromatic (2.5 m)
Medium-resolution	ASTER	8 November 2003	3 multi-spectral (15 m)
Medium-resolution	AVNIR	13 February 2010	4 multi-spectral (10 m)

applying to Beijing metropolitan region and Ruili city, Yunan province, respectively.

In Vietnam, lots of investment on settlement expansion but few measures have been taken to see how the environmental impact of such development in the long-term. Particularly, Saigon South city has been greatly developed since 2000. As urban development is driven mainly by market force (Huynh, 2015; Nguyen, Samsura, van der Krabben, & Le, 2016), more and more houses, commercial blocks and roads invade the wetlands. Are they located on natural water collection points or blocking the natural surface flow? The on-going changes have contributed more flood incidents in the area? Remote sensing monitoring is obviously a solution to address this question, but what would be the most suitable remote sensing image resolutions for identification of the changes? As any Southeast Asian cities, HCMC landscape is complex (Ellis & Ramankutty, 2008), which caused a serious mix-pixel problem in mapping (Small, 2005). Selection of the right spatial resolutions, therefore, is critical to measure the changes correctly.

In this study, we experimented different image resolutions with suitable pixel-based and object-based approaches. We focused on a newly transformed and developed area in the south of HCMC including Districts 4 and 7, which are experiencing the regular flood during and after heavy rain. In the following, Section 2 describes the study area and collected data in further details followed by methodology described in Section 3. We report the findings in Section 4 prior drawing concluding remarks in Section 5.

2. Data collection and study area

The study area was a southern part of HCMC that has been experiencing the rapid expansion of South Saigon city and the followers on the wetlands in last decades. The wetlands here play the critical role in holding rain runoff and releasing it slowly into the river. As over 50% of the land within the city is less than 2 m above sea level, the city is susceptible to more frequent flooding. We covered some areas of districts 4 and 7, and the most focused area for studying within this region was delineated with terrain analysis, which is described in Section 3.1. The study area well represents the transition of city development and transformation. District 4 was an old development defined as a peri-urban area before the 90s, it has been dramatically transformed and become an important connection between core urban areas (Districts 1 and 4) to newly developed areas of South Saigon City in District 7. Extensive development has been observed in the late 90s till now, hence, our analyzed time-frame was between 2000 and 2012. The HCMC map is shown in Fig. 1, highlighting the exact location of the study area.

Digital Elevation Model (DEM) was created from elevation points that were collected from topographic maps scale 1:2000. The exact location of flooding hot-spots in our study area was collected from the Steering Center of Urban Flood Control program of HCMC for 1997, 2005, 2010 and 2011 in addition to the field visit in 2012. The main remote sensing dataset collected is shown in Table 1. We experimented the remote sensing data analysis with 3 different levels of resolutions to investigate the most suitable resolutions for mapping of our study areas, a typical example of Vietnam cities.

We carried out the field visits during dry and raining days along with the brief interview with local communities in 2012. The field visit collected samples for both training and validation purposes. The team went back to revisit the study areas 5 times more. We collected 125 field-trip points some of which are as illustrated in Fig. 2, and extracted 154 points from Google Earth 2003. Validation was, on one hand, to check the accuracy of image classification. It was to examine the urbanization process in the study area against the natural process, on the other hand.

Separately, training samples were delineated directly from satellite

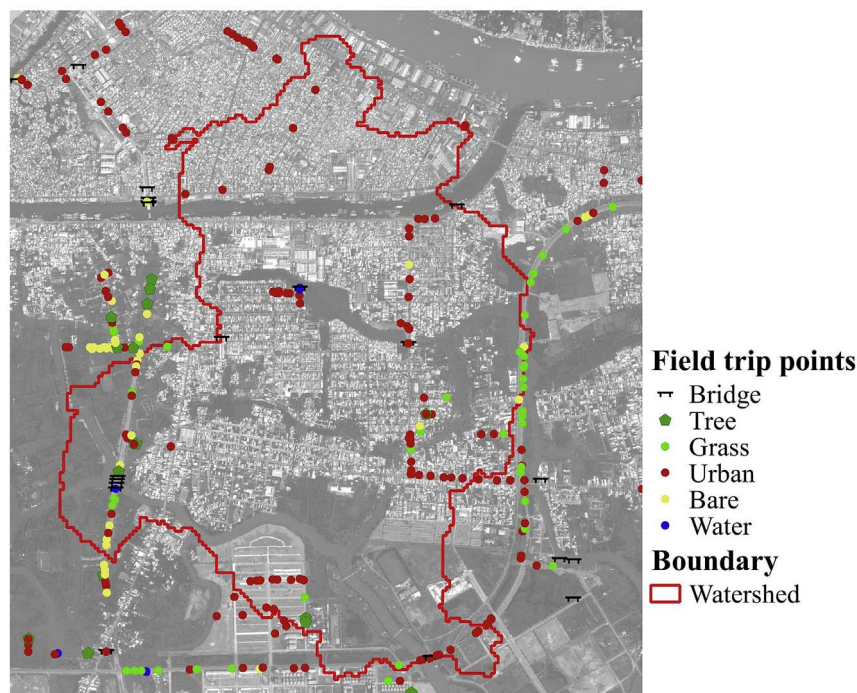


Fig. 2. Illustration of field survey points used for validation.

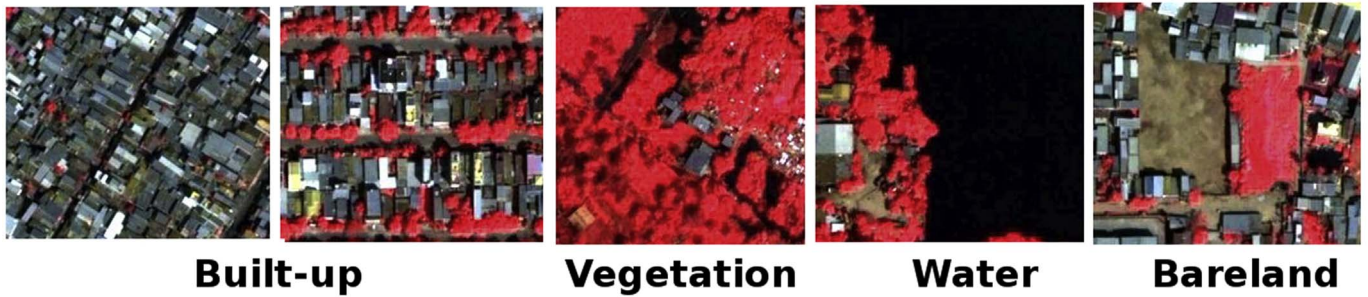


Fig. 3. Examples of training samples in the study area.

images cross-checking with the ground information for 2009 and 2010 images, and with Google Earth for 2003 images. Fig. 3 illustrates the samples of typical landcover types in our study areas such as bare land, built-up, water, and vegetation. The selected samples scattered across our study area and the minimum size is about 200 m² for medium resolution SPOT or ASTER, and 100 m² for high-resolution Quickbird or Worldview.

3. Methodology

3.1. Terrain analysis

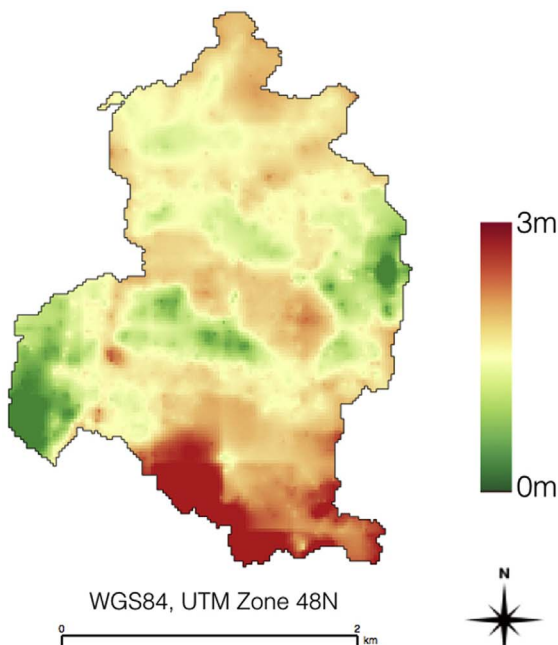
Open-source geospatial tools, QGIS and GRASS, were adopted for terrain analysis. From elevation points of topographic maps scale 1:2000, DEM image with the resolution 20 × 20 m was derived by using bilinear spline interpolation with Tikhonov regularization in GRASS software (the command: *v.surf.bspline*). Based on the generated DEM, the watershed boundaries and accumulation lines were calculated in GRASS software (the command: *r.watershed*). The *r.watershed* is watershed basin analysis program which assigns flow direction for each DEM grid cell, assigns flow accumulation per cell and delineates the

DEM into sub-basins based on the flow accumulation threshold set by the user (Neteler & Mitasova, 2008). The purpose of this step was to reveal the natural process of water flow on the terrain surface, which was then used to examine the newly built-up areas in the study area over the last 10 years.

The selected study area consists of 3 sub-basin areas lying on both districts 4 and 7, which have the boundaries as shown in Fig. 1. Fig. 4 presents the DEM of the study area and its corresponding flow accumulation. During the period of study 2000–2010, on-going changes occurred in the area and there was mixture of old and new built up areas here. The total area is 5,943,467 (m²). With elevation range 0–3 m, this area is at high risk of flooding in the future due to climate change.

Advanced high resolution of satellite images was provided at a high bit depth. Due to the limitation of computer capability, it was impossible to analyze the original huge data of Quickbird and Worldview in the 16-bit format. Quickbird and WorldView image acquired in 11-bit dynamic range but stored in 16-bit format, these images were compressed to 8-bit format yet retaining the similar spectral signatures. Following a simple linear conversion, $newDN = DN(2^8 - 1)/(2^{11} - 1)$ where *DN* stands for the digital number, the output histogram retained

(a) Digital Elevation Model



(b) Flow accumulation

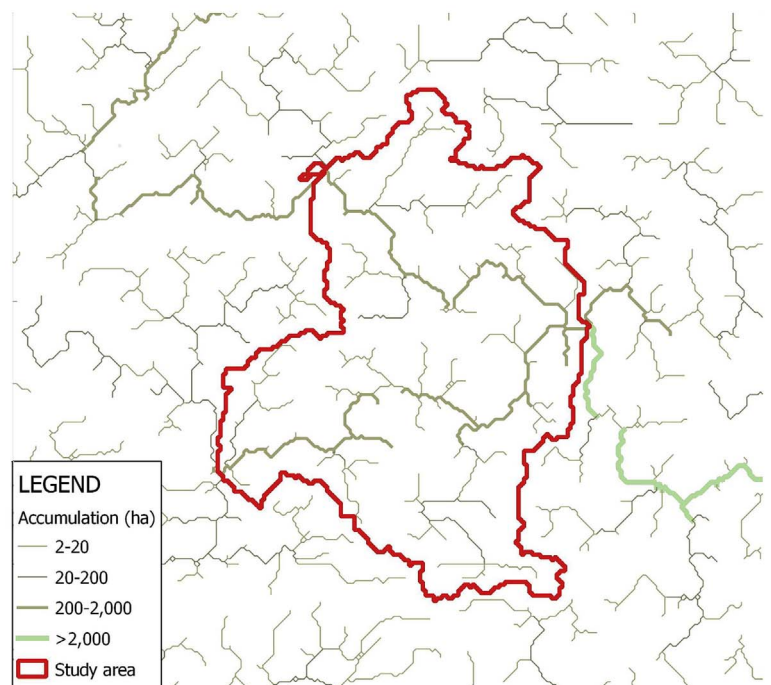


Fig. 4. (a) Digital Elevation Model (DEM) and (b) Flow accumulation of the study area.

Histograms of Band 1 Worldview image

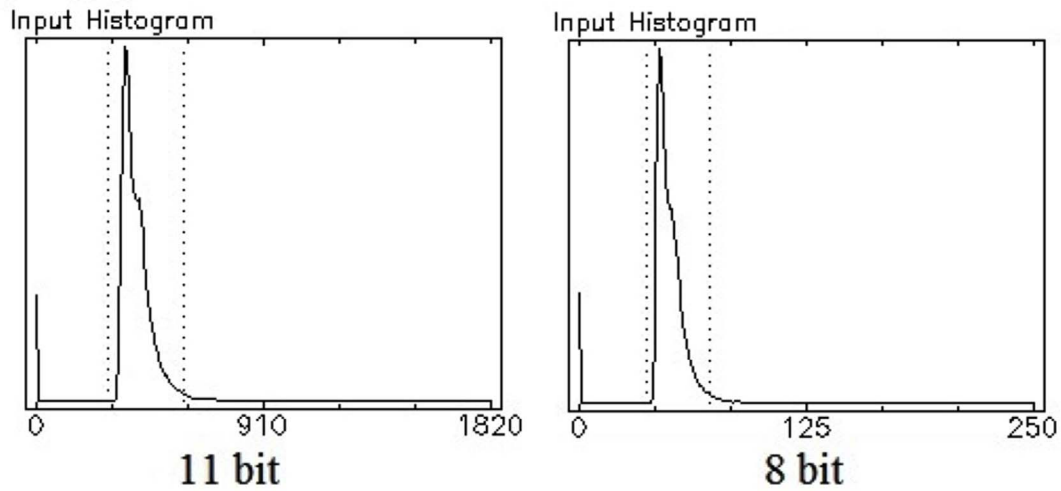


Fig. 5. Histograms of Band 1 Worldview image.

the similar shape to that of the input histogram, e.g. an example of band 1 of Worldview image is illustrated in Fig. 5. In further details, we checked carefully the reflectance behavior of different roof types, which also confirmed the good match between the input and output spectral reflectance curves after conversion (Fig. 6).

3.2. Image classification

Maximum likelihood (ML) has been commonly used, however recently Support Vector Machines (SVM) receives more attention (Mountrakis, Im, & Ogole, 2011). SVM proved to be effective in

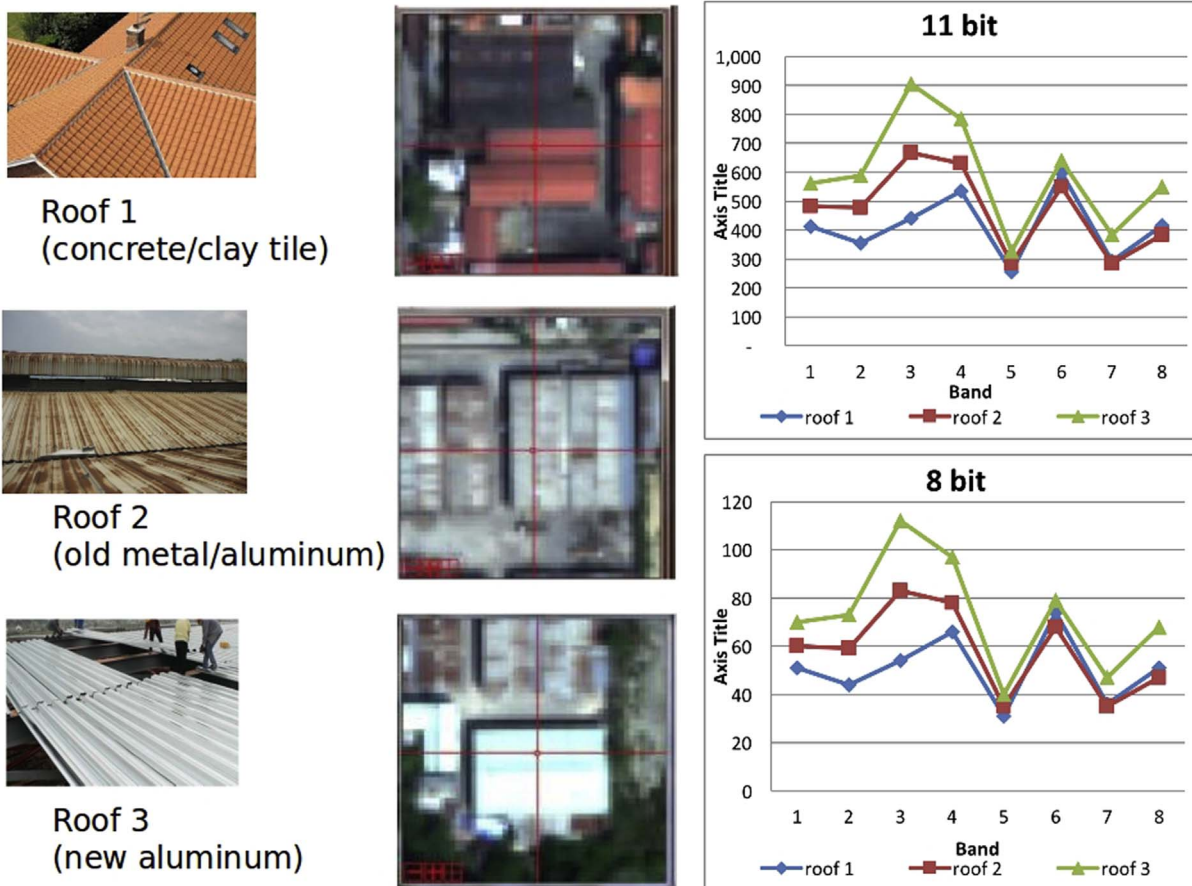


Fig. 6. Spectral reflectance curves of building roofs.

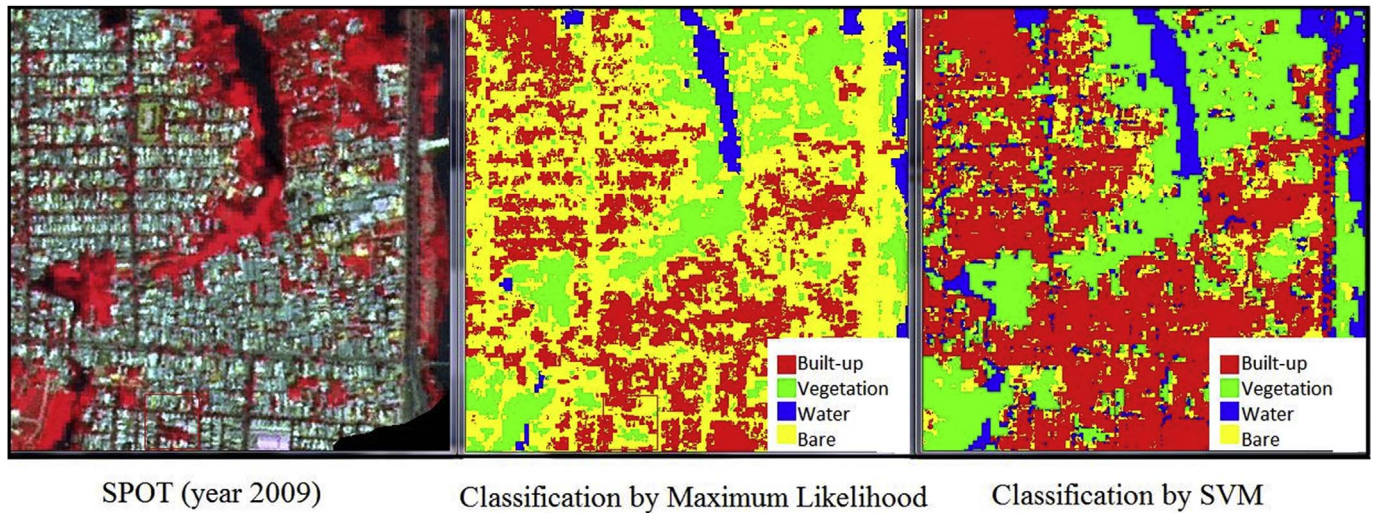


Fig. 7. Comparison between Maximum likelihood and Support Vector Machines classifiers.

handling the classification of complex areas (Griffiths, Hostert, Gruebner, & van der Linden, 2010), and it performs better than ML (Ma et al., 2017). In a previous experiment with another city in Vietnam (Pham, Raghavan, & Pawar, 2010), we also found the better suitability of SVM, following which we did a test as illustrated in Fig. 7. Using the same Region of Interests (ROIs), the SPOT image was classified by SVM and ML for comparison. It confirmed that the SVM produced a better accuracy than that by ML for our study area. We decided to adopt SVM

in this study. Following the recent development of remote sensing image classification, object-based and pixel-based were used accordingly, very high-resolution images were segmented prior to SVM classification to ensure the process was based on the object, not pixels.

4. Result and discussion

We started the classification with highest resolution images,

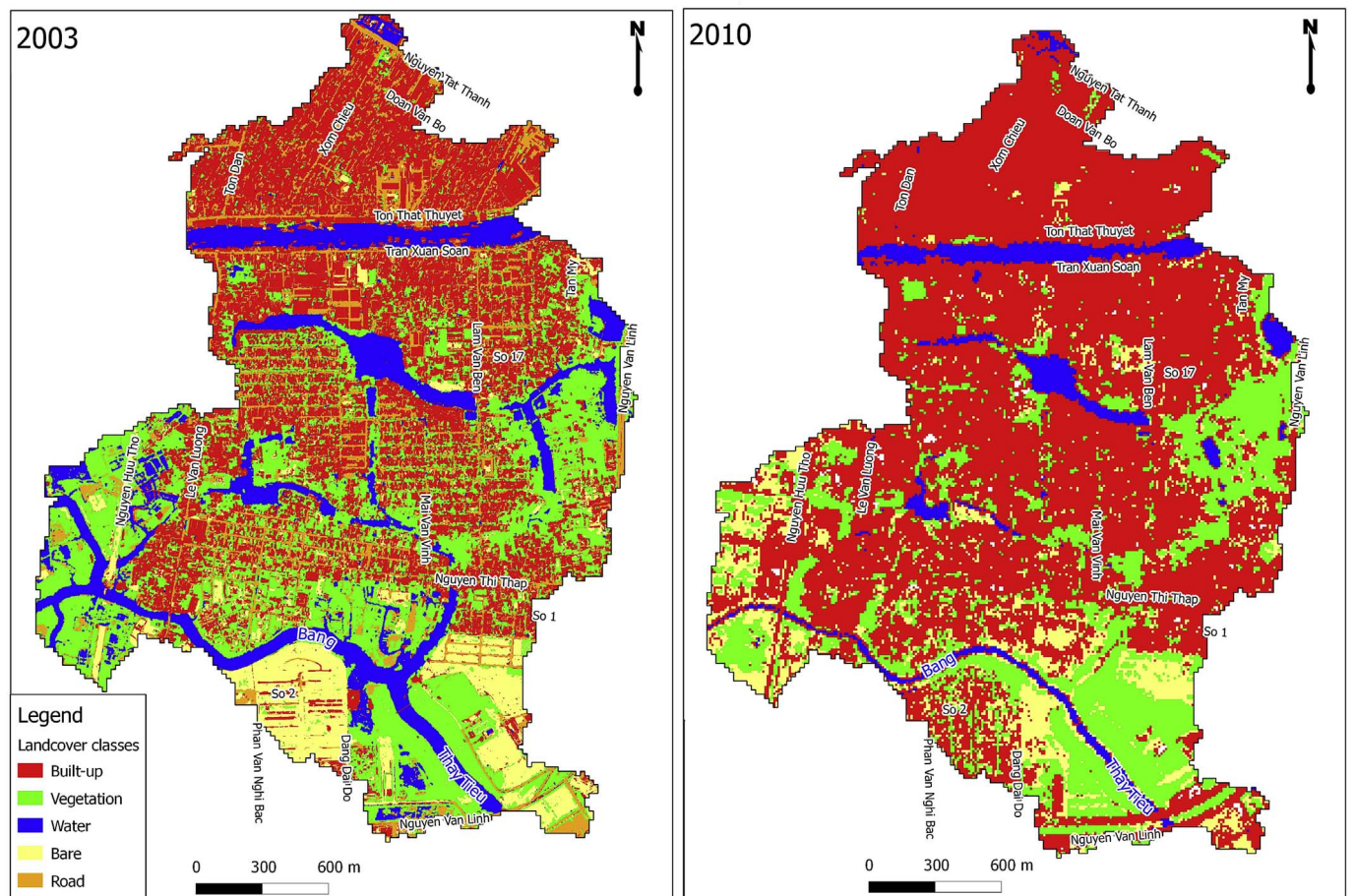


Fig. 8. Classified images from Quickbird images (2003) and Worldview-2 (2010).

WorldView-2 and QuickBird images. The following classes were defined: bare, built-up 1 (blocks of highly dense houses), built-up 2 (blocks of bigger and less dense houses), water (rivers, streams, and lakes), vegetation (grasses, parks), and road. As aforementioned, Quickbird and Worldview-2 were segmented prior to classification. We adopted the Fx module of ENVI, which runs in 2 steps: *Find Objects* and *Extract Objects*. Fx module is the combined process of segmenting an image into regions of pixels, computing attributes for each region to create objects and classifying the objects based on those attributes, to extract features (ITT Visual Information Solutions, 2008). The scale level is the critical parameter in the segmentation process, i.e. *Find Objects* step. After running a number of experiments, we found 60% of scale level in Segment process and 50% of scale level in Merge process

Table 2
Classified results from QuickBird (2003) and Worldview-2 (2010).

	Quickbird 2003 (m ²)	Worldview 2010 (m ²)	Change area (m ²)
Bare	547,908	169,165	-378,744
Road	740,960	615,840	-125,120
Built-up1	1,691,241	1,054,926	-636,315
Built-up2	614,592	2,304,605	1,691,013
Vegetation	1,589,635	1,138,307	-451,329
Water	759,952	660,446	-99,505

Table 3
The confusion matrix of the Worldview 2010 classification.

		Classification				
		Built-up	Bare	Water	Veg.	Sum
Survey	Built-up	76	0	0	2	78
	Bare	9	4	0	0	13
	Water	1	0	11	1	13
	Veg	9	0	0	13	22
Sum		95	4	11	16	126
Overall accuracy		82.53%				
Kappa coefficient		0.79				

Table 4
The confusion matrix of the QuickBird 2003 (0.6 m) classification.

		Classification				
		Built-up	Bare	Water	Veg.	Sum
Survey	Built-up	65	0	1	2	68
	Bare	0	12	3	2	17
	Water	6	2	19	1	28
	Veg	1	0	6	21	28
Sum		72	15	29	25	141
Overall accuracy		82.98%				
Kappa coefficient		0.81				

Table 5
The detailed changes between classes in 2003 and 2010 at sub-meter resolution.

Class	QuickBird 0.6 m 2003 (m ²)				
	Built-up	Veg.	Water	Bare	Class total
Worldview2010	Built-up	2,692,017	780,517	152,459	3,575,003
	Veg.	211,480	639,366	125,812	1,076,658
	Water	117,718	66,418	452,353	636,489
	Bare	24,579	103,334	29,328	157,241
Class total	3,045,794	1,589,635	759,952	547,908	5,943,289
Class changes	353,777	950,269	307,599	535,986	
Image difference	929,573	-451,319	-99,509	-378,745	

are suitable to form most of the objects in this particular study area. Following the suggestion in section 3.2, we applied SVM for classification in *Extract Objects* step.

The results of the classification were shown in Fig. 8 and Table 2, with overall accuracy 82.53% and Kappa coefficient 0.79 for Worldview 2010 (Table 3) and 82.98% and 0.81 for QuickBird 2003 (Table 4). There was the reduction of areas of Built-up 1 and Road classes, due to the ambiguity (and unclear definition) in the reality of low- and high-density built-up areas and road. When combining 3 of them into a built-up class, built-up area showed a clear expansion of 929,578 m², whereas areas of other class were shrunk.

Table 5 further illustrates the change between landcover classes from 2003 to 2010. About 11.6% (353,777m²) of the 2003 built-up land was converted to other landcover types as a result of the urban transformation. However, the built-up took much larger areas from others when expanding. In 2010, the increasing Built-up areas consist of the areas converted from Vegetation (780,517m²), Bare (350,374m²) and Water (152,459m²) classes, which is about 32.28% of total built-up area in 2010. It confirmed that the impervious surface increased in this study area, especially in the south of the study area (District 7) as shown in Fig. 9. In addition, we observe that from 1,589,635m² of vegetation in 2003, only 639,366m² or 40.22% remained in 2010. The loss was mainly due to the expansion of built-up and a lesser portion became bare land and water. A direct comparison shows 451,319m² of vegetation has gone, a bit smaller than the above number as a certain amount of built-up, water and bare land has converted to vegetation.

Using very high-resolution image, we can separate the road and the other built-up areas (houses, concrete surface) (Fig. 10). As shown in this Fig. 10, the increasing of blocks of houses displayed very clearly. However, the higher resolution image, the more mixing between shadow and water classes. Additional processing needs to be carried out to re-assign shadow pixels to their correct land-cover classes. In this study area, since the shadow pixels account a very small percentage of water bodies, those are neglected in our change detection.

At the lower resolution (2.4–2.5 m), we used QuickBird original multi-spectral and SPOT images. Pixel-based classification with SVM was adopted with 4 specified classes: Built-up, Bare, Water, and Vegetation. We achieved overall accuracy 82.96% and Kappa coefficient 0.80 for SPOT 2009 (Table 6) and 80.14% and 0.77 for QuickBird 2003 (Table 7). Fig. 11 presents the classification results and Table 8 showed the statistical changes in which the areas of Built-up and Vegetation classes increased. It is a bit different with the previous result due to different spatial resolutions and the SPOT image was taken in 2009 instead of 2010. The effect of spatial resolution is as illustrated in Fig. 12, i.e. lower spatial resolution is unable to present some small details and hence it influenced the overall classification result. With this resolution, it is obvious that the classified result was not in detail in comparison with that of previous very high-resolution data, and it is difficult to extract the road of 5–10 m widths and covered by trees. However, it is acceptable for built-up detection, the change of built-up can be shown as the built-up region and not in blocks of houses (Fig. 13).

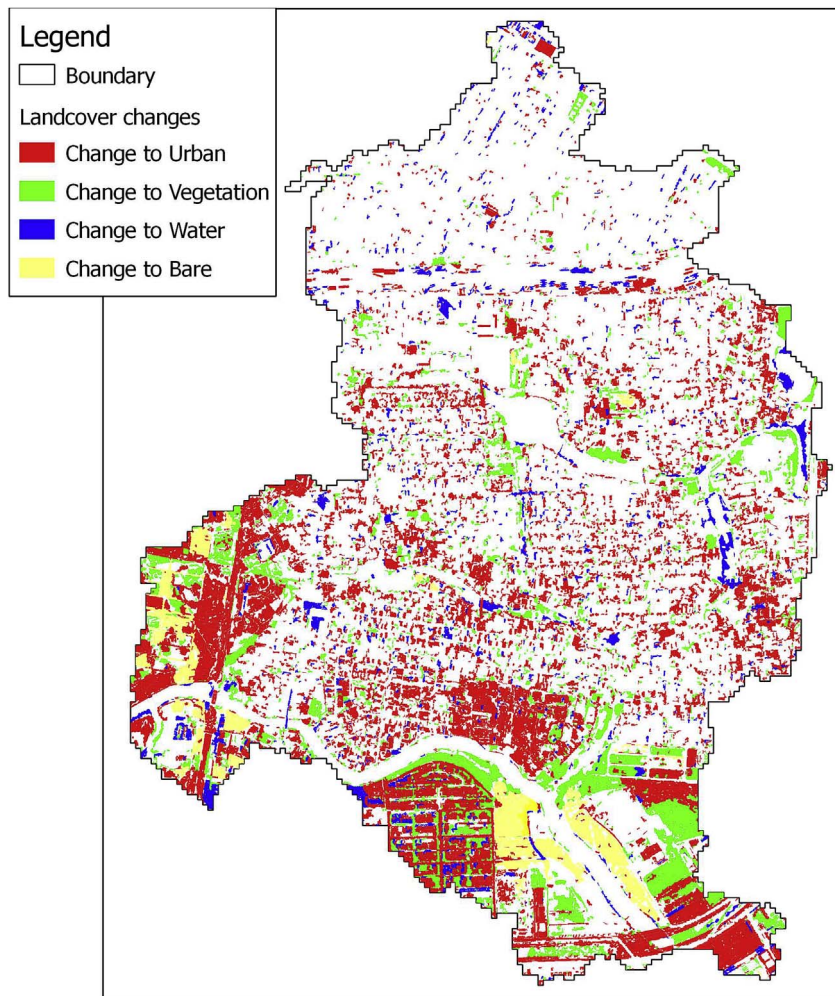


Fig. 9. Landcover changes.

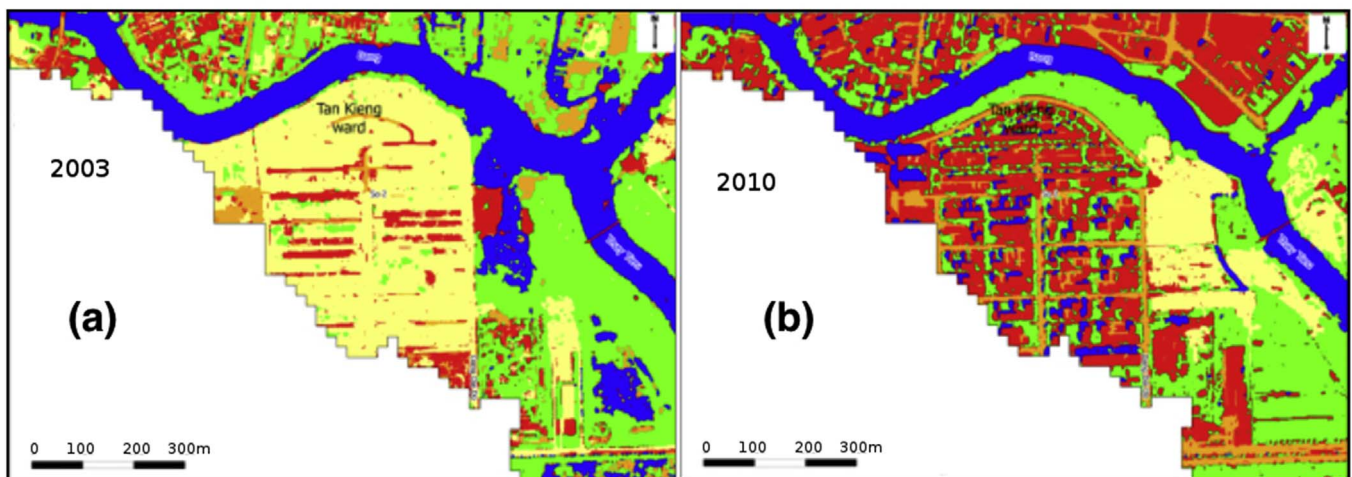


Fig. 10. Landcover classes in Tan Kieng ward a) from QUICKBIRD (2003) and b) WORLDVIEW (2010).

Table 6
The confusion matrix of the SPOT 2009 classification.

		Classification				Sum
		Built-up	Bare	Water	Veg.	
Survey	Built-up	75	0	2	3	80
	Bare	8	4	0	2	14
	Water	2	0	13	0	15
	Veg	6	0	0	20	26
Sum		91	4	15	25	135
Overall accuracy		82.96%				
Kappa coefficient		0.80				

Table 7
The confusion matrix of the QuickBird 2003 (2.4 m) classification.

		Classification				Sum
		Built-up	Bare	Water	Veg.	
Survey	Built-up	65	0	1	2	68
	Bare	0	12	1	4	17
	Water	6	2	16	4	28
	Veg	1	1	6	21	28
Sum		72	15	24	30	141
Overall accuracy		80.14%				
Kappa coefficient		0.77				

Classification of medium resolution satellite images (10–15 m resolution) produced not very good result (Fig. 14), e.g. some small river branches disappeared in AVNIR image as show in Fig. 15, though quantitative accuracy is quite acceptable. The overall accuracy 76.98% and Kappa coefficient 0.72 was achieved for AVNIR 2010 and 82.27% and 0.79 for ASTER 2003 (see Tables 9 and 10). Due to coarse spatial resolution, the road networks were unable to extract and small patches of built-up areas were easily merged into bigger bare land or vegetation areas. Overall, however, the statistical result illustrates the increasing of Built-up area that was converted mainly from Bare and Vegetation areas (Table 11).

The classification results infer that only less than 1 m spatial resolution is suitable to map and monitor the on-going urban changes, which are the present status of many areas in Ho Chi Minh City, Vietnam. About 2.5 m resolution is reasonably good for delineating the built-up areas as a whole, not in blocks of buildings. That may be useful to delineate the extent of built-up areas. The use of 2009 image instead of 2010 prevents some further investigation of spatial resolution effect as some real landcover change definitely took place during that fast-growing and transformation period.

By visual comparison, it seems that similar multi-temporal landcover maps were produced at different spatial resolutions. However, spatial resolutions have great influence on the quantitative measures of landcover types and hence, computed different values of landcover changes, as illustrated in Fig. 12. Let's look into the measures of each landcover types on Quickbird 0.6 m and Quickbird 2.4 m images, which

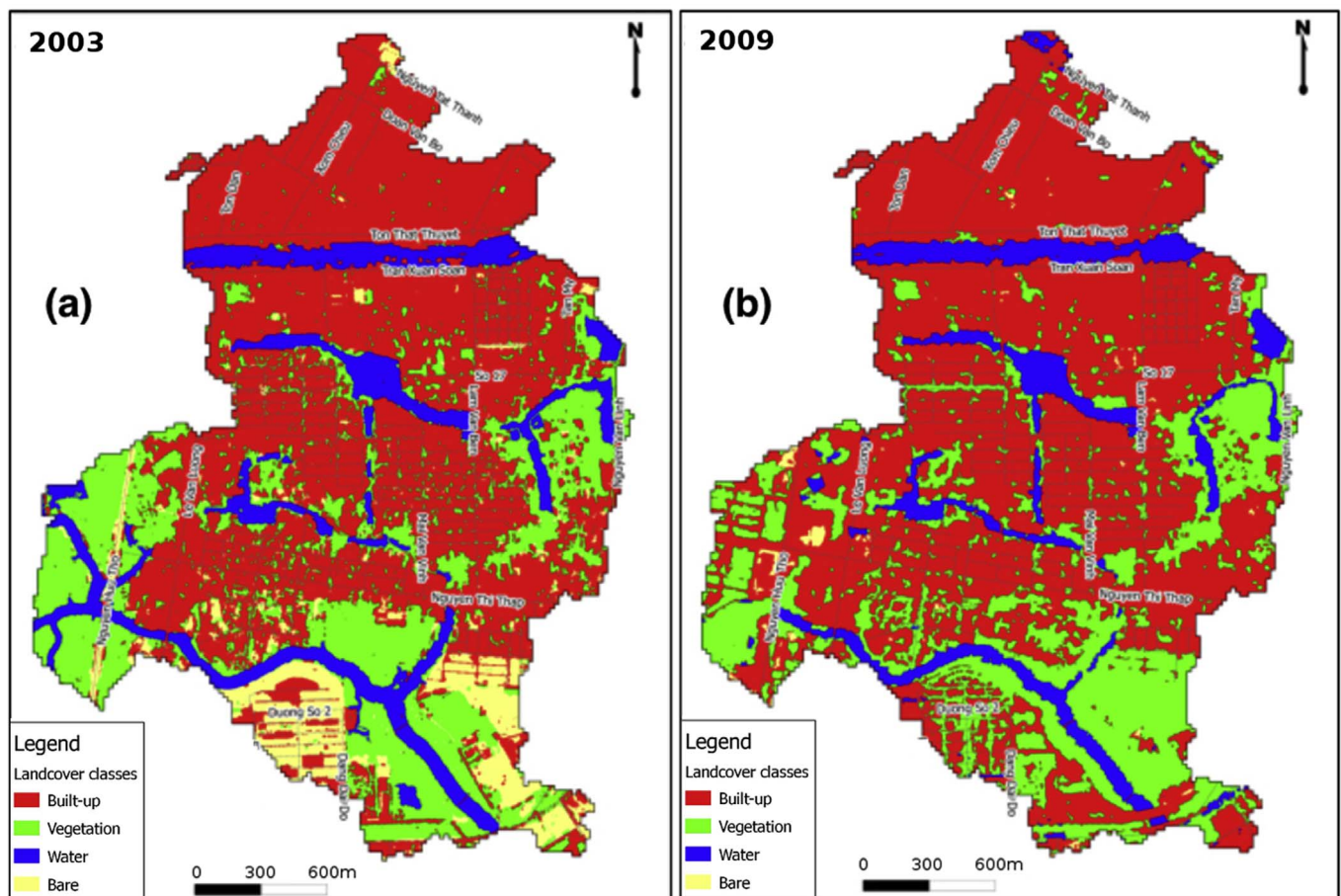


Fig. 11. Classified images from Quickbird 2.4 m (2003) and SPOT 2.5 m (2009).

Table 8
The detailed changes between classes in 2003 and 2009 at 2.5 m resolution.

Class		QuickBird 2.4 m 2003 (m^2)				Class total
		Built-up	Veg.	Water	Bare	
SPOT2009	Built-up	3,020,907	517,012	76,666	215,752	3,830,337
	Veg.	365,507	789,258	123,085	250,606	1,528,456
	Water	44,099	52,301	431,073	7776	535,248
	Bare	9700	18,749	2246	4429	35,124
Class total		3,440,212	1,377,320	633,070	478,564	
Class changes		419,305	588,061	201,997	474,134	
Image difference		397,325	154,835	-97,407	-443,134	

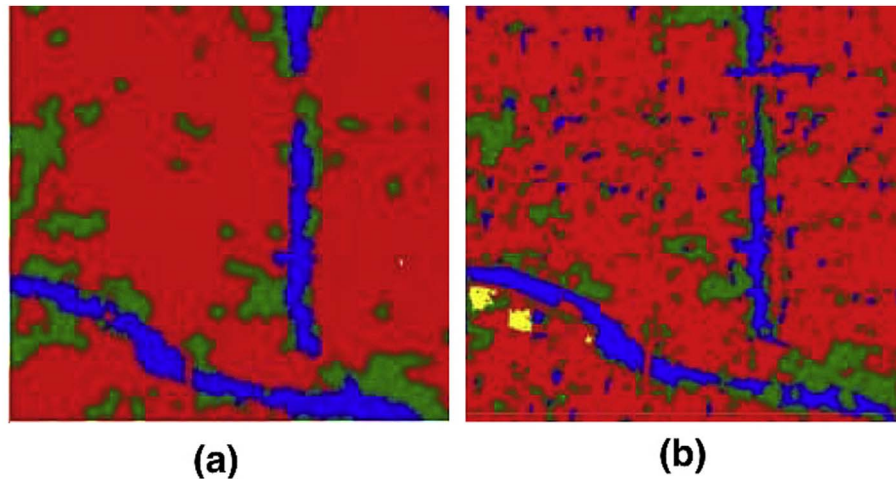


Fig. 12. Comparison of classified results from a) SPOT 2.5 m and Worldview 0.5 m

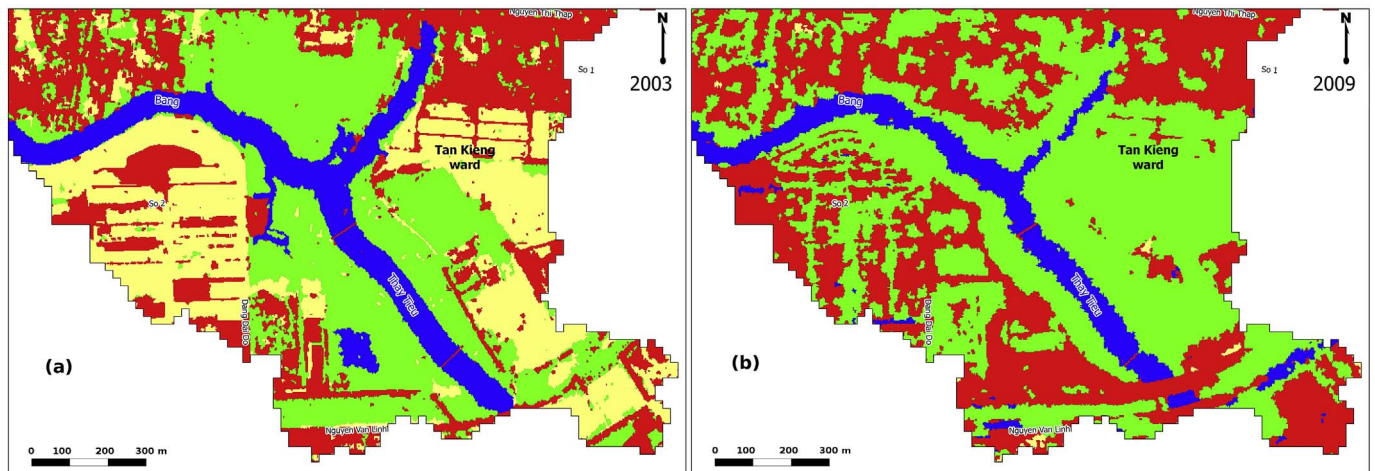


Fig. 13. Landcover classes in Tan Kieng ward a) from QUICKBIRD 2.4 m (2003) and b) SPOT 2.5 m (2009).

came from the same sensor. The differences between them are $-394,418(m^2)$ built-up, $212,316(m^2)$ vegetation, $126,882(m^2)$ water and $69,344(m^2)$ bare land, which are -12.95% , 13.36% , 16.70% and 12.66% differences, respectively. The extensive changes to built-up areas took place in the study area, beyond these differences, therefore,

the results showed consistently the increase of built-up area in three different level of spatial resolutions but it is not the case for other landcover types.

The detection of landcover change confirmed that the impervious surface expands significantly in this area, 30% increase from 3,045,794

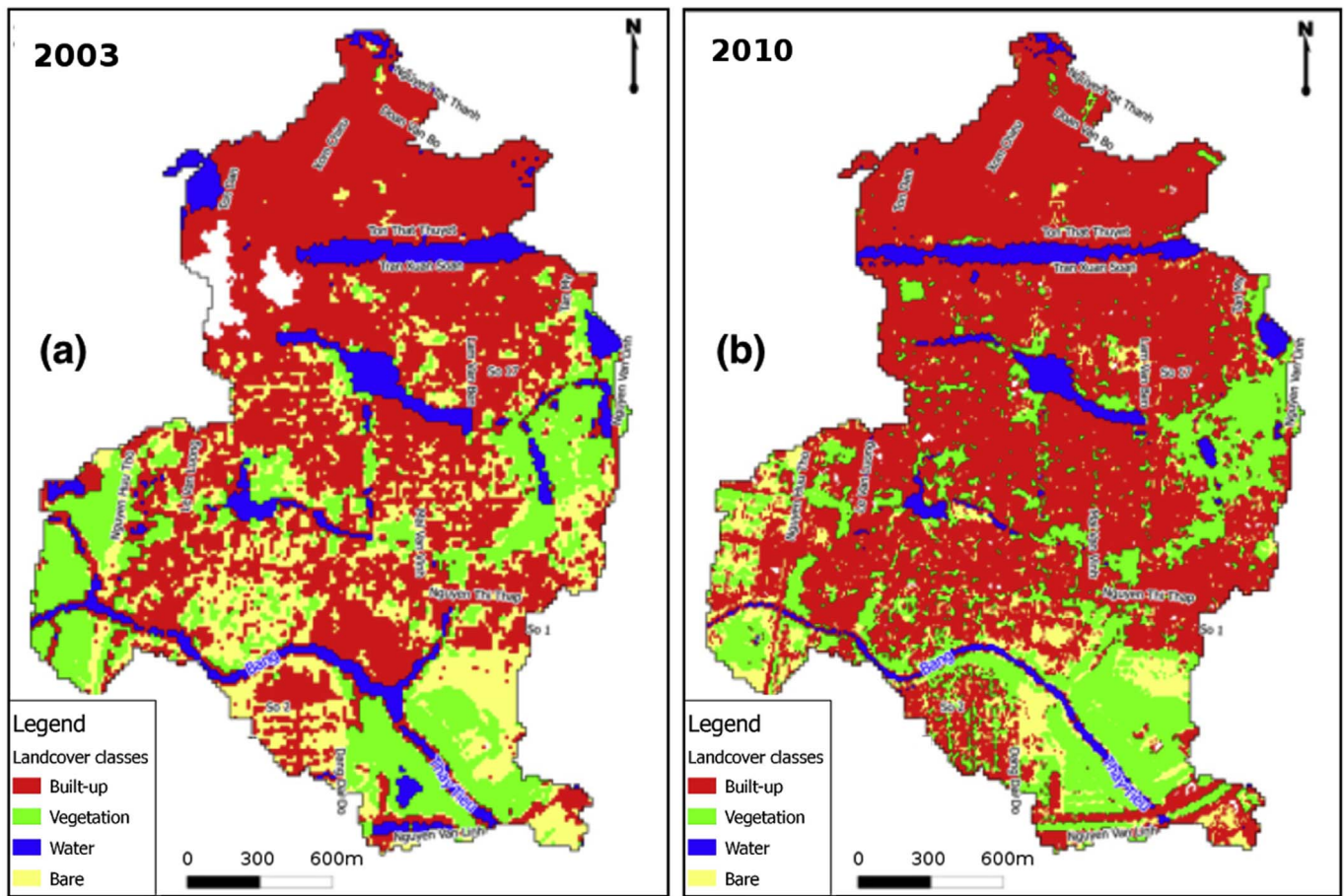


Fig. 14. Classified images from ASTER 15 m (2003) and AVNIR 10 m (2010).

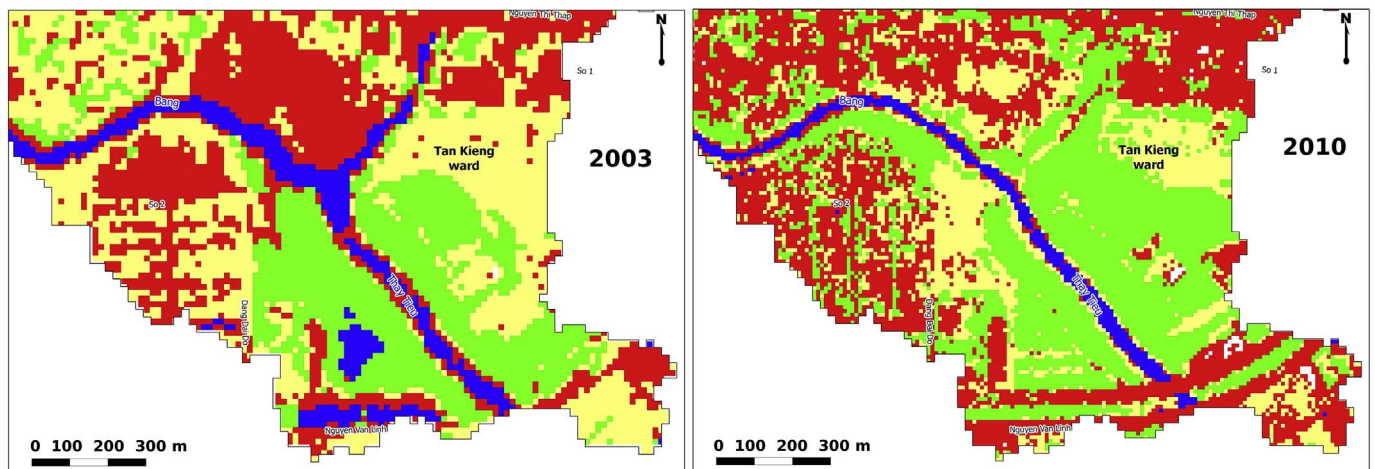


Fig. 15. Landcover classes in Tan Kieng ward a) from ASTER 15 m (2003) and b) from AVNIR 10 m (2010).

(m^2) in 2003 to 3,975,367 (m^2) in 2010 with sub-meter images and about 22% with medium resolution 15 m images. The expansion rate is in line with the result by Kontgis et al. (Kontgis et al., 2014), which used time-series Landsat images to monitor peri-urbanization in HCMC in 1990–2012. Particularly, our study area was marked as a combination of high change rate from 6.9% to 13.1% to greater than 24% in

Kontgis et al. (Kontgis et al., 2014). About 28% of vegetation disappeared highlighted the severe issue of losing wetland and croplands in the area, a typical example of many similar areas in HoChiMinh city.

Referring to the ground observation, in the years between 1997 and 2006, the flooding areas concentrated mostly in District 4 which locate on Doan Van Bo, Ton Dan, Xom Chieu streets (blue lines in Fig. 16b).

Table 9
The confusion matrix of the AVNIR 2010 classification.

		Classification				
		Built-up	Bare	Water	Veg.	Sum
Survey	Built-up	67	9	0	1	77
	Bare	4	8	0	0	12
	Water	1	0	11	3	15
	Veg	7	4	0	11	22
Sum		79	21	11	15	126
Overall accuracy		76.98%				
Kappa coefficient		0.72				

Table 10
The confusion matrix of the ASTER 2003 classification.

		Classification				
		Built-up	Bare	Water	Veg.	Sum
Survey	Built-up	61	4	1	2	68
	Bare	4	13	0	0	17
	Water	5	3	19	1	28
	Veg	2	1	2	23	28
Sum		72	21	22	26	141
Overall accuracy		82.27%				
Kappa coefficient		0.79				

Later, from 2009 to 2012, floods have been increased more in both districts which locate on Nguyen Huu Hao and Hoang Dieu (further north and outside of the study area), Huynh Tan Phat (further to the east and outside of the study area), and Nguyen Thi Thap streets (inside of study area, District 7)(red line in Fig. 16b). Further checking in Fig. 16c revealed that the flood areas found in the top and middle of the study area, are in low terrain areas and on the accumulate lines. Rapid change to built-up occurred in the south and southeast of the study area, the new constructions are mainly in the high area (> 2 m). Another new built-up area on the west is on the lower terrain but the natural river nearby (just outside the study area to the left) plays a significant role in easing the pressure. However, all changes contributed to the increment of the flood on nearby lowland areas, e.g. Nguyen Thi Thap street.

Remote sensing images, topography map and ground observation data provided the clear illustration of how the expansion of sealed soil areas can increase the pressure on natural water flow in our study area. However, without the information of drainage systems, we were unable to investigate further if the current infrastructure has been developed to cope with the problem? An integrated analysis of both terrain accumulation line network and drainage network would be an interesting extended study to reveal the real water flow in the area.

Kontgis et al (Kontgis et al., 2014). also highlighted that the total population of HCMC was nearly 12 million by 2012. Fast population growth accelerates the extraction of underground water and contributes to land subsidence with the rate 5–15 mm/year (Minh et al., 2015). Taking into account the sea level rise, all cause the increasing inundation problems in the city. Flood, among many others, is just one direct and obvious incidence as the consequences of fast urbanization without following an appropriate urban planning in the context of climate change. The long-term environmental and ecological impacts of transforming wetland to built-up areas have not been assessed and taken into consideration (Douglass & Huang, 2007). The fast

Table 11
The detailed changes between classes in 2003 and 2010 at medium spatial resolution.

Class		ASTER 2003 (m ²)				
		Built-up	Veg.	Water	Bare	Class total
AVNIR 20-10	Built-up	2,565,000	270,450	159,525	735,075	3,730,050
	Veg.	222,975	552,825	75,825	270,225	1,121,850
	Water	55,125	3600	212,850	3150	274,725
	Bare	204,075	171,900	29,700	210,150	615,825
Cloud		11,925	4725	900	9000	26,550
Class total		3,059,100	1,003,500	478,800	1,227,600	
Class changes		494,100	450,675	265,950	1,017,450	
Image difference		670,950	118,350	-204,075	-611,775	

development is driven by the market force and speeds up beyond the capability of administrative planning and management here as well as other cities in the similar stage of development.

5. Conclusion

Remote sensing observation revealed the evidence of fast urbanization via mapping impervious surface. Focusing on a selected hot-spot of fast growth in last decade, remote sensing mapping with three different levels of resolution confirmed over 25% increase of built-up in the area. Sub-meter spatial resolution proved to be the most suitable resolution for the typical complex landscape of HCMC and other similar developing cities. High-resolution 2.5 m is not suitable for mapping in details like narrow roads and individual buildings, but suitable to map the whole block of buildings. We suggest using the 2.5 m image to delineate built-up extent whereas sub-meter image to map the hotspot of on-going changes in details. Medium resolution image produced an unsatisfactory result for our study area. Further investigation needs to be done for investigating the quality of acquired images and perhaps, more suitable classification approach.

Most of the newly developed built-up areas found located on the higher land and experienced no flood. However, it is quite clear that more built-up areas on natural wetland increase the pressure back to the old areas and hence more flood occurred in the lower land areas when raining or even flood tide. While the improvement of drainage systems in core urban areas hardly keeps pace with the urbanization rate, sealing soil here prevents the natural process of handling excess water when heavy raining. The evidence of land subsidence and sea level rise from other research and ground observation add more serious environmental concerns on the development of south and south-east areas of HCMC.

Remote sensing technologies today can timely provide both synoptic and details views of anthropogenic activities that are an important input to a holistic urban planning and management. The outcome of this study suggests the effective use of suitable spatial resolution for remote sensing mapping of growing city in developing countries. In the further study, we will expand the study site, integrating the drainage system into the water flow simulation, to provide a better link between land-use change and flood in the city that can play a reference for developing different urban growth scenarios. Moreover, all relevant factors such as land subsidences, climate-related measures, landuse change will be taken into consideration for better understanding the urban development stories.

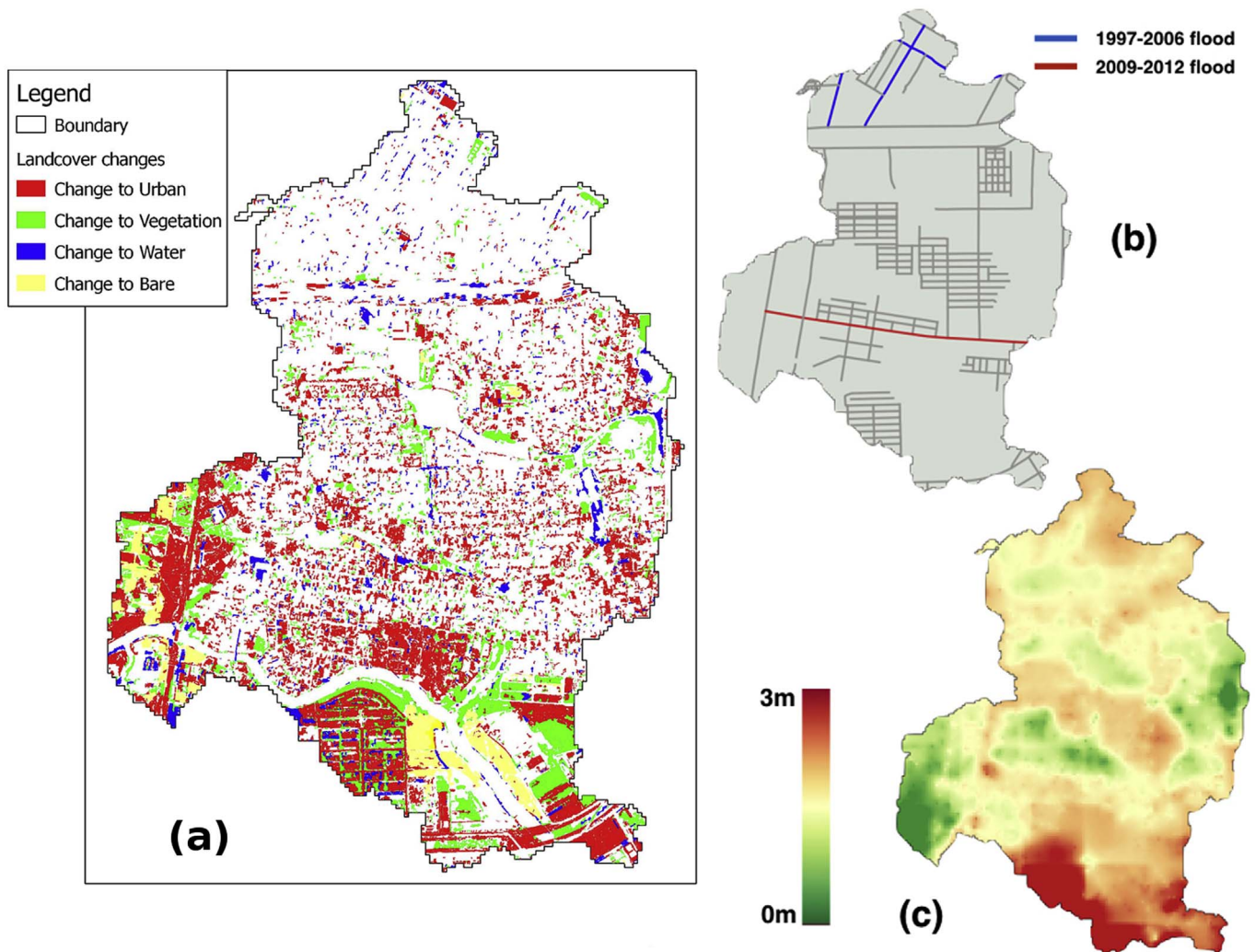


Fig. 16. (a) Landcover changes and (b) Flooding streets and (c) DEM.

Acknowledgement

This research is partly supported by the Project "Using remote sensing, GIS and mathematical model to assess climate change in Southern Vietnam" (code T.NCCB-HD.2012-G/03) of Vietnam's National Foundation for Science and Technology Development (NAFOSTED). We are also grateful for the financial support from the Faculty of Science, University of Nottingham, Malaysia campus. The recorded flood locations were provided by the Steering Center of Urban Flood Control program of Ho Chi Minh city.

References

- ADB (2010). *Ho chi minh city - adaptation to climate change*. Tech. rep. Asia Development Bank.
- Blaschke, T. (2010). Object based image analysis for remote sensing. *ISPRS Journal of Photogrammetry and Remote Sensing*, 65(1), 2–16.
- Blaschke, T., Hay, G. J., Kelly, M., Lang, S., Hofmann, P., Addink, E., et al. (2014). Geographic object-based image analysis – towards a new paradigm. *ISPRS Journal of Photogrammetry and Remote Sensing*, 87(0), 180–191.
- Douglass, M., & Huang, L. (2007). Globalizing the city in southeast asia: Utopia on the urban edge—the case of phu my hung, saigon. *IJAPS*, 3(2), 1–42.
- Ellis, E. C., & Ramankutty, N. (2008). Putting people in the map: Anthropogenic biomes of the world. *Frontiers in Ecology and the Environment*, 6(8), 439–447.
- Esch, T., Himmler, V., Schorcht, G., Thiel, M., Wehrmann, T., Bachofer, F., et al. (2009). Large-area assessment of impervious surface based on integrated analysis of single-date landsat-7 images and geospatial vector data. *Remote Sensing of Environment*, 113(8), 1678–1690.
- Gamba, P., Dellà"Acqua, F., & Dasarathy, B. V. (2005). Urban remote sensing using multiple data sets: Past, present, and future. *Information Fusion*, 6(4), 319–326.
- Gómez, C., White, J. C., & Wulder, M. A. (2016). Optical remotely sensed time series data for land cover classification: A review. *ISPRS Journal of Photogrammetry and Remote Sensing*, 116, 55–72.
- Griffiths, P., Hostert, P., Gruebner, O., & van der Linden, S. (2010). Mapping megacity growth with multi-sensor data. *Remote Sensing of Environment*, 114(2), 426–439.
- Grimm, N. B., Faeth, S. H., Golubiewski, N. E., Redman, C. L., Wu, J., Bai, X., et al. (2008). Global change and the ecology of cities. *Science*, 319(5864), 756–760.
- Gu, H., Li, H., Yan, L., Liu, Z., Blaschke, T., & Soergel, U. (2017). An object-based semantic classification method for high resolution remote sensing imagery using ontology. *Remote Sensing*, 9(4), 329.
- Hanh, V. T. H. (2006). Canal-side highway in ho chi minh city (hcmc), vietnam—issues of urban cultural conservation and tourism development. *Geojournal*, 66(3), 165–186.
- Huang, X., Zhang, L., & Zhu, T. (2014). Building change detection from multitemporal high-resolution remotely sensed images based on a morphological building index. *IEEE Journal of Selected Topics in Applied Earth Observations and Remote Sensing*, 7(1), 105–115.
- Hu, X., & Weng, Q. (2009). Estimating impervious surfaces from medium spatial resolution imagery using the self-organizing map and multi-layer perceptron neural networks. *Remote Sensing of Environment*, 113(10), 2089–2102.
- Huynh, D. (2015). The misuse of urban planning in ho chi minh city. *Habitat International*, 48, 11–19.
- Kontgis, C., Schneider, A., Fox, J., Saksena, S., Spencer, J. H., & Castrence, M. (2014). Monitoring peri-urbanization in the greater ho chi minh city metropolitan area. *Applied Geography*, 53, 377–388.
- Leichtle, T., Geiß, C., Wurm, M., Lakes, T., & Taubenböck, H. (2017). Unsupervised change detection in vhr remote sensing imagery—an object-based clustering approach in a dynamic urban environment. *International Journal of Applied Earth Observation and Geoinformation*, 54, 15–27.
- Lu, D., Li, G., & Moran, E. (2014). Current situation and needs of change detection techniques. *International Journal of Image and Data Fusion*, 5(1), 13–38.
- Lu, D., Moran, E., & Hetrick, S. (2011). Detection of impervious surface change with multitemporal landsat images in an urban-rural frontier. *ISPRS Journal of Photogrammetry and Remote Sensing*, 66(3), 298–306.
- Lu, D., & Weng, Q. (2004). Spectral mixture analysis of the urban landscape in

- Indianapolis with Landsat ETM+ imagery. *Photogrammetric Engineering & Remote Sensing*, 70(9), 1053–1062.
- Ma, L., Li, M., Ma, X., Cheng, L., Du, P., & Liu, Y. (2017). A review of supervised object-based land-cover image classification. *ISPRS Journal of Photogrammetry and Remote Sensing*, 130, 277–293.
- Minh, D. H. T., Van Trung, L., Toan, T. L., et al. (2015). Mapping ground subsidence phenomena in Ho Chi Minh City through the radar interferometry technique using ALS data. *Remote Sensing*, 7(7), 8543–8562.
- Mountrakis, G., Im, J., & Ogole, C. (2011). Support vector machines in remote sensing: A review. *ISPRS Journal of Photogrammetry and Remote Sensing*, 66(3), 247–259.
- Mountrakis, G., & Luo, L. (2011). Enhancing and replacing spectral information with intermediate structural inputs: A case study on impervious surface detection. *Remote Sensing of Environment*, 115(5), 1162–1170.
- Neteler, M., & Mitasova, H. (2008). *Open source GIS: A grass GIS approach, the international series in engineering and computer science, Vol. 773*.
- Nguyen, T. B., Samsura, D. A. A., van der Krabben, E., & Le, A.-D. (2016). Saigon-Ho Chi Minh City. *Cities*, 50, 16–27.
- Pham, T. M. T., Raghavan, V., & Pawar, N. J. (2010). Urban expansion of Can Tho City, Vietnam: A study based on multi-temporal satellite images. *Geoinformatics*, 21(3), 147–160.
- Pu, R., & Landry, S. (2012). A comparative analysis of high spatial resolution Ikonos and WorldView-2 imagery for mapping urban tree species. *Remote Sensing of Environment*, 124, 516–533.
- Scalenghe, R., & Marsan, F. A. (2009). The anthropogenic sealing of soils in urban areas. *Landscape and Urban Planning*, 90(1), 1–10.
- Schneider, A., Mertes, C., Tatem, A., Tan, B., Sulla-Menashe, D., Graves, S., et al. (2015). A new urban landscape in East–Southeast Asia, 2000–2010. *Environmental Research Letters*, 10(3), 034002.
- Small, C. (2005). A global analysis of urban reflectance. *International Journal of Remote Sensing*, 26(4), 661–681.
- UN (2014). *World Urbanization Prospects*. Tech. Rep. United Nations.
- Van de Voorde, T., Jacquet, W., & Canters, F. (2011). Mapping form and function in urban areas: An approach based on urban metrics and continuous impervious surface data. *Landscape and Urban Planning*, 102(3), 143–155.
- Vu, T., Matsuoka, M., & Yamazaki, F. (2007). Dual-scale approach for detection of tsunami-affected areas using optical satellite images. *International Journal of Remote Sensing*, 28(13–14), 2995–3011.
- Webster, D., McElwee, P., & Worldbank (2009). Urban adaptation to climate change: Bangkok and Ho Chi Minh City as test beds. *Fifth urban research symposium, cities and climate change: Responding to an urgent agenda* (pp. 28–30).
- Weng, Q. (2007). *Remote sensing of impervious surfaces*. CRC Press.
- Weng, Q. (2012). Remote sensing of impervious surfaces in the urban areas: Requirements, methods, and trends. *Remote Sensing of Environment*, 117(0), 34–49.
- Wieland, M., & Pittore, M. (2016). Large-area settlement pattern recognition from Landsat-8 data. *ISPRS Journal of Photogrammetry and Remote Sensing*, 119, 294–308.
- Yu, W., Zhou, W., Qian, Y., & Yan, J. (2016). A new approach for land cover classification and change analysis: Integrating backdating and an object-based method. *Remote Sensing of Environment*, 177, 37–47.
- Zhang, J., & Kerekes, J. (2011). Unsupervised urban land-cover classification using WorldView-2 data and self-organizing maps. *Geoscience and Remote Sensing Symposium (IGARSS), 2011* (pp. 150–153). IEEE International. IEEE.
- Zhang, H., Zhang, Y., & Lin, H. (2012). A comparison study of impervious surface estimation using optical and {SAR} remote sensing images. *International Journal of Applied Earth Observation and Geoinformation*, 18(0), 148–156.
- Zhang, Y., Zhang, H., & Lin, H. (2014). Improving the impervious surface estimation with combined use of optical and {SAR} remote sensing images. *Remote Sensing of Environment*, 141(0), 155–167.
- Zhu, Z. (2017). Change detection using Landsat time series: A review of frequencies, preprocessing, algorithms, and applications. *ISPRS Journal of Photogrammetry and Remote Sensing*, 130, 370–384.